

References

- [1] Graziano, V., Gerchman, S.E., Schneider, D.K. and Ramakrishnan, V., *Nature* (1994) **368**, 351-354.
- [2] Lasters, I., Wyns, L., Muyltermans, S., Baldwin, J.P., Poland, G.A. and Nave, C., *Eur. J. Biochem.* (1985) **151**, 283-289.
- [3] Williams, S.P., Athey, B.D., Muglia, L.J., Schappe, R.S., Gough, A.H. and Langmore J.P., *Biophys. J.* (1986) **49**, 233-248.
- [4] Baldwin, J.P., Bosely, P.G., Bradbury, E.M. and Ibel, K., *Nature* (1975) **253**, 245-249.
- [5] Widom, J. and Klug, A., *Cell* (1985) **43**, 207-213.
- [6] Thoma, F., Koller, T. and Klug A., *J. Cell Biol.* (1979) **83**, 403-427.
- [7] Staynov, D.Z., *Int. J. Biol. Macromol.* (1983) **5**, 3-9.
- [8] Belikov, S. and Karpov, V., *Febs Lett.* (1998) **441**, 161-164.
- [9] Allan, J., Hartman, P.G., Crane-Robinson, C. and Aviles, F.X., *Nature* (1980) **288**, 675-679.
- [10] Lambert, S.J., Muyltermans, S., Baldwin, J., Kilner, J., Ibel, K. and Wins, L., *Biochem. Biophys. Res. Commun.* (1991) **179**, 810-816.
- [11] Baldwin, J.P., *Curr. Opin. Struct. Biol.* (1992) **2**, 78-83.
- [12] Hayes, J.J. and Wolffe, A.P., *Proc. Natl. Acad. Sci. USA* (1993) **90**, 6415-6419.
- [13] Kilner, J., Ph.D. Thesis (John Moores University 1993).
- [14] Lambert, S.J., Nicholson, J.M., Chantalat, L., Reid, A.J., Donovan, M.J. and Baldwin, J.P., *Acta Cryst. D* (1999) **55**, 1048-1051.
- [15] Chantalat, L., Nicholson, J.M., Lambert, S.J., Reid, A.J., Donovan, M.J. and Baldwin, J.P., (submitted).
- [16] Luger, K., Mader, A.W., Richmond, R.K., Sargent, D.F. and Richmond, T.J., *Nature* (1997) **389**, 251-260.

Real Time FTIR and WAXS Studies of the Drawing Behaviour of Polyethylene Terephthalate Fibres

A.C. Middleton¹, R.A. Duckett¹ and I.M. Ward¹,
A. Mahendrasingam², C. Martin²

¹ IRC in Polymer Science and Technology, University of Leeds, Leeds LS2 9JT.

² Department of Physics, University of Keele, Keele ST5 5BG.

The development of molecular orientation and crystallisation has been studied during uniaxial drawing of polyethylene terephthalate (PET) films followed immediately by subsequent taut-annealing at the drawing temperature. The behaviour was monitored in real time throughout both drawing and annealing using dynamic FTIR spectroscopy and in situ WAXS measurements using the Daresbury Synchrotron Radiation Source.

The IR spectra were analysed using curve reconstruction procedures developed previously, and showed that orientation of the phenylene groups and the trans glycol conformers occurred before significant gauche-trans conformational changes could be seen. The onset of crystallisation, defined as the point that the crystalline 105 reflection could be first observed using WAXS, was not found to correlate with any specific change in the proportions of trans and gauche isomers nor with any feature on the stress-strain curve. However, it was clear that for these comparatively low strain rates, crystallisation occurred during the drawing process, whilst the cross-head was moving, and the draw ratio was increasing.

Introduction

There is considerable evidence from studies of the solid phase deformation of polyethylene terephthalate and related polyesters to show that some aspects can be very well represented by the deformation of a molecular network. In particular, it appears that a molecular network is formed in melt spinning of fibres as the spun yarn cools in the threadline. Provided that no crystallisation occurs, the oriented spun yarn behaves like a frozen stretched rubber, so that a network draw ratio can be defined and quantitative stress-optical measurements can determine the molecular parameters of the network, such as the density of molecular

entanglements [1]. Further stretching, either by cold drawing below the glass transition temperature T_g , or hot drawing above T_g , involves further stretching of the molecular network. Where crystallisation occurs, the network draw ratio can be determined by curve matching *i.e.* fitting the strain hardening part of the room temperature true stress-true strain curves to the template for an isotropic unoriented spun yarn by a simple shift on the true strain axis (Figures 1(a) and

1(b)). It has been shown that properties such as modulus, tenacity and birefringence can then be related to the total network draw ratio [2] where the spin line stretch is added to the subsequent drawing stretch (Figures 2(a) and 2(b)).

Related structural measurements on the oriented PET have been undertaken by wide-angle and small angle X-ray diffraction and by a range of spectroscopic

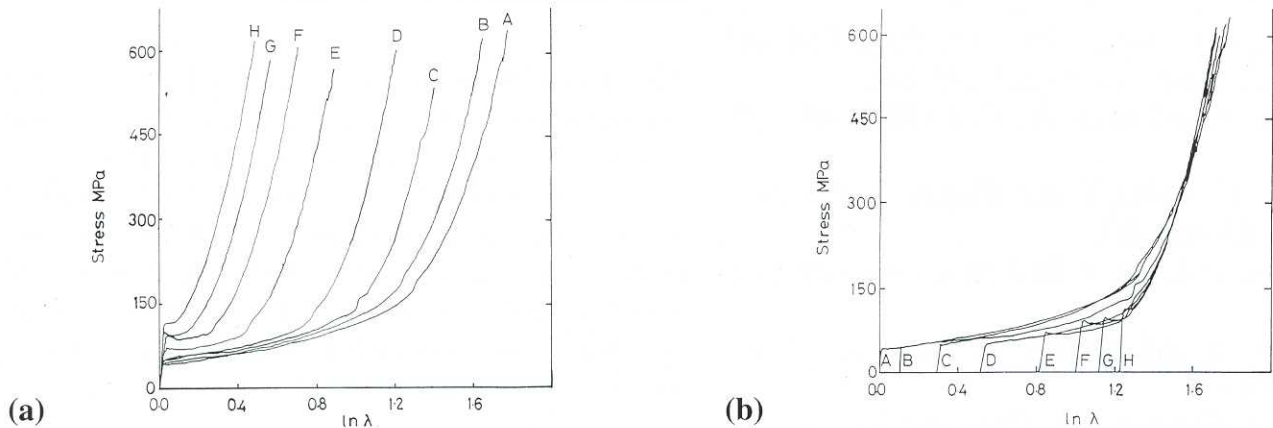


Figure 1: (a) True stress-strain curves for spun yarns. A to H is increasing spun yarn orientation. (b) Matching of true stress-strain curves for spun yarns.

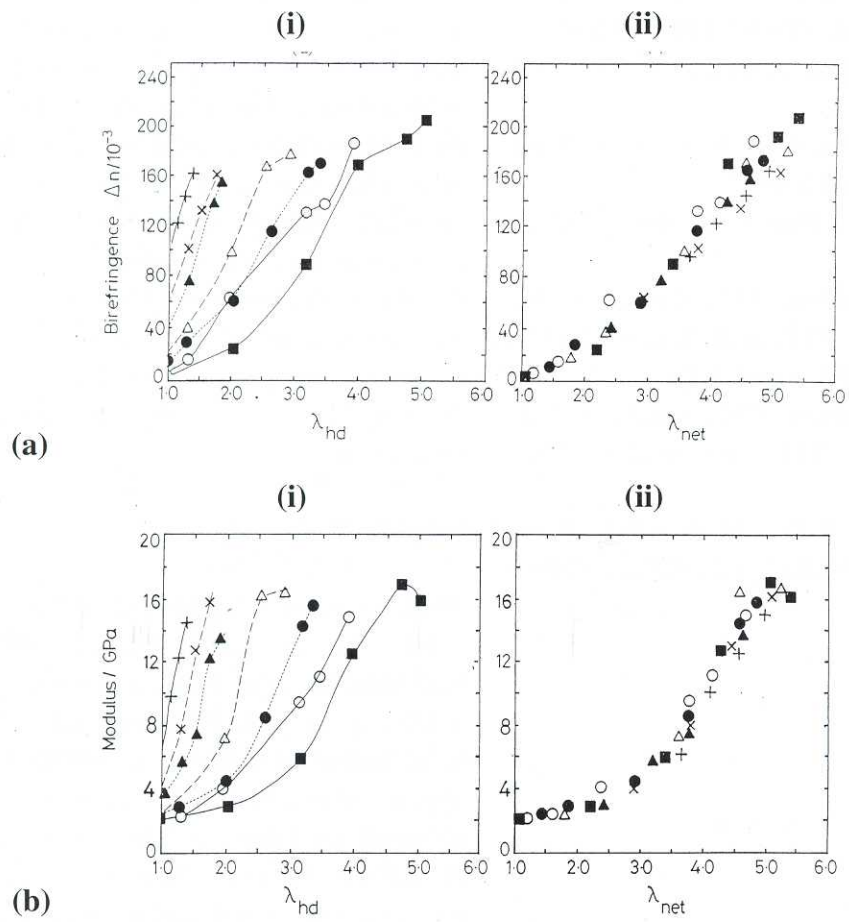


Figure 2: (a) Birefringence vs actual hot draw ratio λ_{hd} (i) and network draw ratio λ_{net} (ii) for spin-drawn yarns and their spun yarn precursors. (b) Initial modulus vs actual hot draw ratio λ_{hd} (i) and network draw ratio λ_{net} (ii) for spin-drawn yarns and their precursors. A = squares, B = hollow circles, C = filled circles, D = hollow triangles, E = filled triangles, F = diagonal crosses, H = crosses, where A to H is increasing spun yarn orientation due to increased wind-up speed)

techniques, including infra-red, Raman and polarised fluorescence spectroscopy and NMR. For high wind-up speed fibres for drawing above T_g with draw ratios greater than about 2.5, crystallisation occurs. At a molecular level the chain conformations which are primarily crumpled *gauche* conformations in the isotropic polymer are transformed into extended *trans* conformations, which exist in the crystalline regions as shown by the crystal structure determined by Bunn and co-workers [3]. The development of molecular orientation and the changes in *trans/gauche* content have also been very successfully modelled by the deformation of a molecular network (Figures 3(a) and 3(b)) [4].

It is remarkable that the correlations between properties and network draw ratio and the simple algorithms developed for the development of molecular orientation and conformational changes appear to be insensitive to the onset of crystallisation. This observation has led to the research described in this article where wide-angle

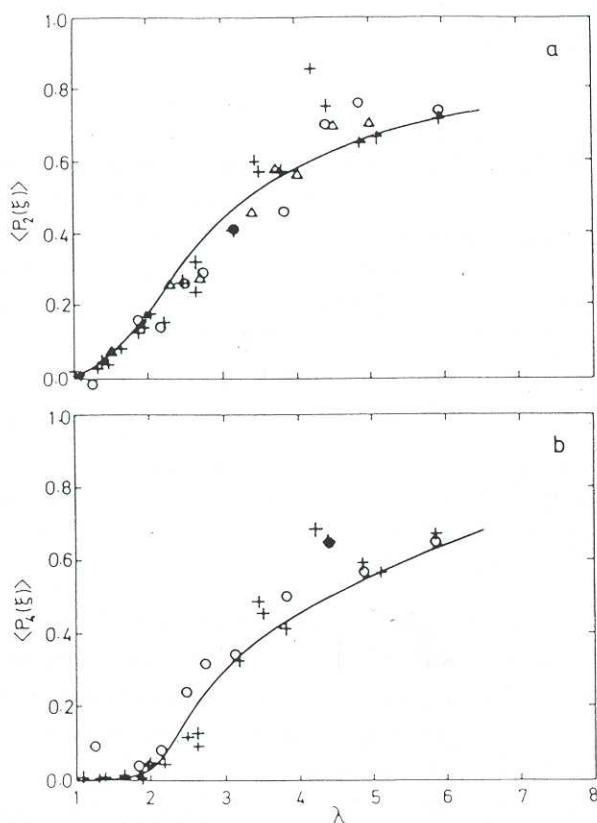


Figure 3: Development of molecular orientation as a function of draw ratio. $\langle P_2(\xi) \rangle$ and $\langle P_4(\xi) \rangle$ are the second and fourth Legendre functions describing molecular orientation. Theoretical predictions = solid line, experimental results from refractive index measurements = triangles, fluorescence measurements = crosses, Raman measurements = circles.

X-ray diffraction measurements made *in situ* during the drawing process are combined with FTIR Raman measurements also made in-line to monitor molecular orientation and *trans/gauche* content.

Experimental

I-R spectroscopy

Polarised I-R spectra were recorded in real-time by drawing samples in a Minimat materials tester mounted on the sample stage of a BOMEM MB-151 FTIR spectrometer. The spectrometer was controlled by a NEC personal computer using commercially available Spectra-Calc software. The chamber was heated by the circulation of hot air and the glass entry and exit windows were replaced with potassium bromide (KBr). Parallel and perpendicular polarisation spectra were recorded on successive samples which underwent identical thermal and mechanical histories. This could be justified because drawing under these conditions was found to be almost perfectly reproducible. A schematic of the Minimat showing the experimental arrangement required for the collection of polarised spectra whilst the sample is both heated and drawn is shown in Figure 4.

WAXS

The samples studied using WAXS were drawn in a purpose built X-ray camera [5,6]. The camera was heated by two heating elements and the air was circulated by wall mounted fans. The camera was mounted on its side and positioned so that the sample was tilted through an angle of 21° towards the

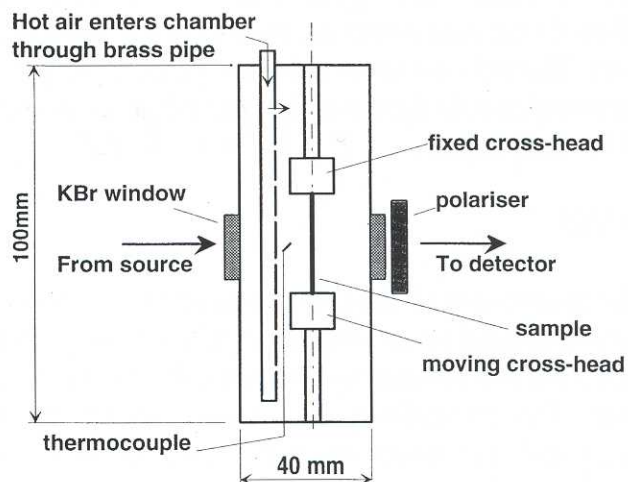


Figure 4: Schematic diagram of temperature chamber for the Minimat material tester mounted on the BOMEM sample stage.

incident beam. The instrumentation required to perform dynamic experiments and collect diffraction patterns in real-time using the Keele camera is discussed fully in [7].

All the real-time WAXS experiments were carried out at the Daresbury SRS. The beam had a monochromated wavelength of 1.488\AA and the current varied from 156 mA to 131 mA during each 24 hour period. The diffraction patterns were collected using a CCD camera. The camera was placed normal to the incident X-ray beam and close to the aluminium foil window in order to minimise air scatter. Unfortunately the size of the detector area and the geometry of the experiment meant that only part of the pattern was recorded. The detector was therefore carefully positioned so that it was able to record both the centre of the diffraction pattern and the $\bar{1}05$ reflection.

Results and Discussion

I-R Spectroscopy

Figures 5(a) and 5(b) show the variation in the *trans* and *gauche* conformer contents and the orientation of the *trans*, *gauche* and benzene ring bands respectively for samples drawn at 80°C and at a cross-head speed of 5mm/min.

The majority of the *gauche* to *trans* conversion occurred whilst the cross-head was moving, but there were also some changes during the annealing period whilst the draw ratio remained constant. It should be noted that the possible variations in the conformer contents at the final draw ratio appear artificially high on these graphs since random scatter in the data will have the same appearance as a genuine trend when all the data points are plotted at the same draw ratio. There do not seem to be any sudden changes in the *trans/gauche* ratio which could relate to the onset of crystallisation.

WAXS

The progression of the crystallisation of each sample was monitored by recording the peak intensity of the reflection and comparing it with the draw ratio at that time. The crystallinity is actually related to the integrated area under the reflection, but, since the Gaussian half width of the reflection underwent very little change during the course of each experiment, a semi-quantitative study can be completed by

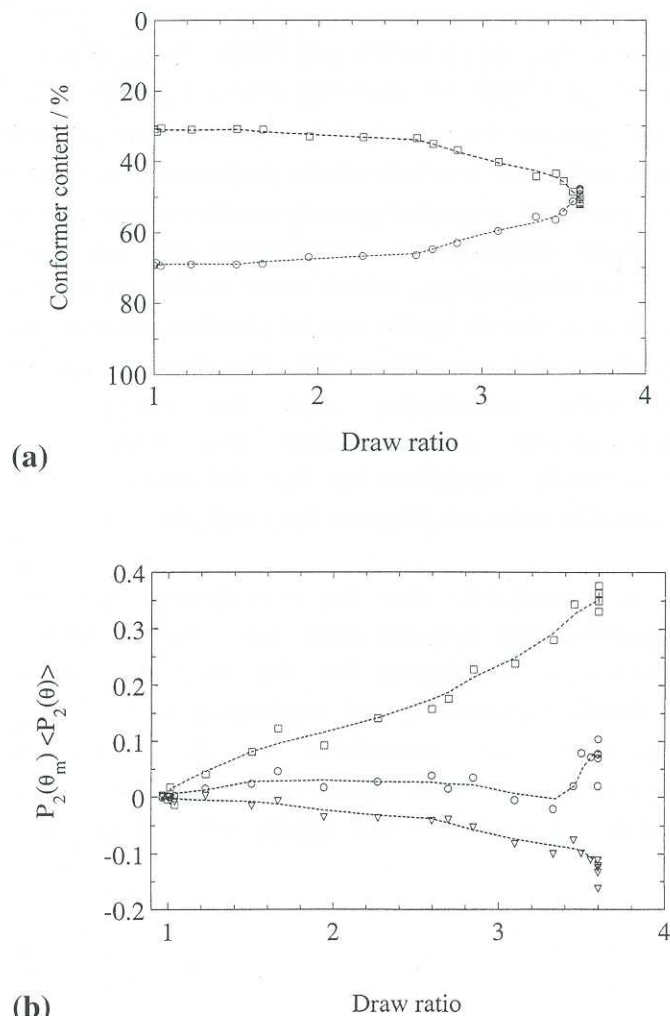


Figure 5: (a) *Trans* (squares) and *gauche* (circles) contents as functions of draw ratio for sample drawn at 80°C and cross-head speed 5mm/min. (b): Orientation of 972cm^{-1} *trans* (squares), $890 + 899 + 906\text{cm}^{-1}$ *gauche* (circles) and $872 + 878\text{cm}^{-1}$ benzene ring band (triangles) as a function of draw ratio for sample drawn at 80°C and 5mm/min.

considering simply the peak intensity. Figure 6 shows the development of the crystalline $\bar{1}05$ peak for samples drawn at 5mm/min.

Crystallisation clearly occurs during the draw. Once it has reached a recordable level, the peak intensity of the azimuthal scan then increases approximately linearly throughout the remainder of the draw. It may be that the development of the crystalline reflection proceeds smoothly from zero in which case the peak may have existed in earlier diffraction patterns without rising clear of the noise. Alternatively the peak behaviour may be as presented here such that the peak initially shows discontinuous growth. This would agree with the hypothesis of other researchers that crystallisation is initiated from many different centres as soon as a critical condition is established

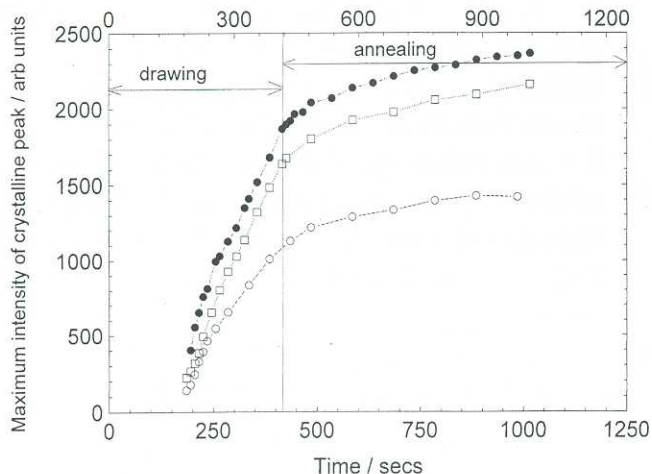


Figure 6: Development of crystalline peak during drawing and annealing of samples drawn at 5mm/min. 85°C thick = hollow circles, 80°C thin = filled circles, 80°C thick = squares.

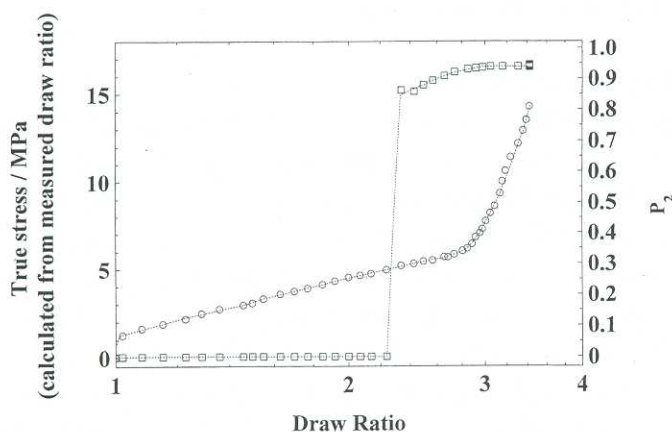


Figure 7: P_2 (squares) and true stress (circles) versus draw ratio for thick samples drawn at 80°C, 5mm/min.

(e.g. the amorphous orientation passes a certain level) [8,9]. Draw ratios at which the reflection first became apparent during each experiment were always close to 2.5 and it was difficult to discern any other trend from the data.

Figure 7 shows the variation of the orientation parameter $\langle P_2(q) \rangle_{105,m}$ and the true stress values with draw ratio for the 200 μ m sample drawn at 80°C and 5mm/min. The orientation parameter has been abbreviated to P_2 in the figure. The point at which a Gaussian curve can first be fitted to the WAXS data does not seem to correspond to any particular feature on the true stress-strain curve and the majority of the draws under all conditions showed a similar lack of correlation between the onset of crystallisation and the true stress vs strain. The orientation of the 105

crystallites is always very high, appearing with values of 0.80 to 0.90 and rising to 0.95 by the end of the annealing period, regardless of the drawing conditions.

The most significant conclusion which can be drawn from the real-time WAXS results is that the crystallisation occurs whilst the cross-head is moving and the draw ratio is increasing. This is further confirmation of recent results by Blundell *et al.* [7]. The crystalline peak was first observed for draw ratios close to 2.5 and no clear trend emerged from the data between the draw ratio and the temperature or speed of drawing. However, the fraction of the final intensity which developed whilst the cross-head was moving showed a definite correlation with the drawing speed and implied that drawing at very high speeds would result in crystalline reflections which developed entirely after the cross-head stopped moving.

Conclusions

The combination of FTIR spectroscopy and WAXS results taken during the drawing and taut annealing of PET film has provided considerable insight into the mechanism of drawing and crystallisation. *Gauche/trans* isomerisation is clearly detectable during drawing, at a rate which increases with increasing draw-rate and decreasing temperature. The orientation of the *trans* conformers also increased in a similar way. The WAXS technique is sensitive only to those *trans* conformers in crystalline regions and these are only detected at draw-ratios above approximately 2.2. When observed, the crystallites are seen to be highly oriented – more oriented than the overall *trans* orientation. The onset of crystallisation as detected by WAXS is not marked by any sudden change in number or orientation of *trans* conformers, nor with any particular feature of the stress-strain curves. There is clear evidence that crystallisation is occurring during the drawing process, although at the higher drawing speeds the majority of the crystallisation observed occurred during the taut-annealing process.

Acknowledgements

A. C. Middleton held an EPSRC CASE studentship sponsored by ICI Films. The authors thank Dr D. J. Blundell and Dr D. MacKerron of ICI Films for their contributions to this research.

References

- [1] Pinnock, P.R. and Ward, I.M., *Trans. Faraday Soc.* (1966) **62**, 1308.
- [2] Long, S.D. and Ward, I.M., *J. Polym. Sci. Polym. Phys. Ed.* (1991) **42**, 1921.
- [3] Bunn, C.W., Daubeny, R. de P. and Brown, C.J., *Proc. Roy. Soc. A* (1954) **10**, 275.
- [4] Nobbs, J.H., Bower, D.I. and Ward, I.M., *J. Polym. Sci. Polym. Phys. Edn* (1979) **17**, 259.
- [5] Mahendrasingam, A., MacKerron, D.H., Fuller, W., Forsyth, V.T., Oldman, R.J. and Blundell, D.J., *Rev. Sci. Instrum.* (1992) **63**, 1097.
- [6] Blundell, D.J., Mahendrasingam, A., MacKerron, D.H., Turner, A., Rule, R., Oldman, R.J. and Fuller, W., *Polymer* (1994) **35**, 3875.
- [7] Blundell, D.J., MacKerron, D.H., Fuller, W., Mahendrasingam, A., Martin, C., Oldman, R.J., Rule, R. and Riekel, C., *Polymer* (1996) **37**, 3303.
- [8] Salem, D.R., *Polymer* (1992) **33**, 3189.
- [9] Salem, D.R., *Polymer* (1992) **33**, 3182.

8th Annual Workshop Prize-Winning Posters

An XRD Study of the Rigid-Rod Polymer Fibre M5 (PIPD)

E.A. Klop and M. Lammers

Akzo Nobel Central Research, P.O.Box 9300, 6800 SB Arnhem, Netherlands.

Introduction

The spinning of rod-like polymer molecules from liquid crystalline solutions has proven to be an effective way of preparing fibres that exhibit high stiffness and tenacity. The high level of molecular orientation already present in the as-spun state can be further increased by heat treatment resulting in materials suitable for high-performance structural applications. This spinning and heat treatment process is used in the production of the rigid-rod polymer fibre poly (*p*-phenylene benzobisoxazole) (PBO). The performance of this fibre (and related fibres) in compression, however, is disappointing, due to the absence of strong interchain bonding. In recent years much effort has been spent on increasing

the lateral strength of rigid rod polymer fibres, often by crosslinking after fibre formation. These efforts were not very successful.

Figure 1 shows the structural formula of the rigid-rod polymer M5, which was discovered in our laboratory [1]. The design of this polymer, with chemical name poly {2,6-diimidazo[4,5-b:4'5'-e]pyridinylene-1,4(2,5-dihydroxy) phenylene}, abbreviated as "PIPD", was motivated by its ability to form intermolecular hydrogen bonds. Fibres spun from a nematic solution of the polymer in polyphosphoric acid not only exhibit a high stiffness and tenacity (330 and 5 GPa respectively), but also a compression strength (1.7 GPa) which exceeds that of any other polymer fibre. Compared with carbon fibre, the material has the advantage of having a very high damage tolerance; moreover, it is an electrical insulator. While the heat-treated material has attractive properties, the as-spun material is interesting as well, as it is highly fire-resistant. The work reported here concerns the structural order both in heat-treated and as-spun M5 fibre.

Heat-treated M5 fibre

The diffraction pattern of heat-treated M5 fibre (Figure 2(a)) shows several reflections on the first three layer-lines, indicating three-dimensional crystalline order. Despite the small number of reflections, it was possible to determine the unit cell parameters and the packing of the polymer molecules, using a diffraction modelling approach. Based on the flat plate diffraction pattern, two models are proposed which have the same lattice (with parameters 12.60 Å, 3.48 Å, 12.01 Å, 90.0°, 108.6°, 90.0°) but different symmetry, *viz.* a triclinic

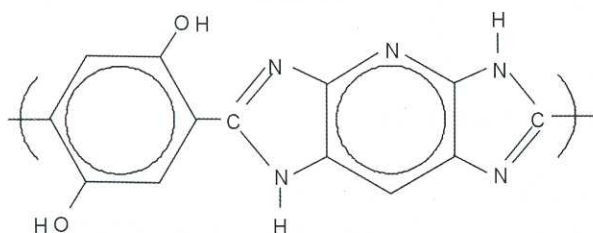


Figure 1: Chemical structure of M5.